Microscopic carrier dynamics of quantum-well-based light storage cells

S. K. Zhang, P. V. Santos,[a] and R. Hey
Paul-Drude-Institut, Hausvogteiplatz 5–7, 10117 Berlin, Germany

A. Garcia-Cristóbal and A. Cantarero
Materials Science Institute, Universidad de Valencia, Burjasot, E-46100 Valencia, Spain

(Received 6 September 2000; accepted for publication 6 November 2000)

The dynamics of storage and recombination of electron–hole pairs in quantum-well-based light memory cells driven by high-frequency electric fields is investigated by spatially and time-resolved photoluminescence spectroscopy. In these cells, a laterally modulated potential is used to ionize and spatially separate photogenerated electron–hole pairs. The temporal and spatial dependence of the carrier dynamics depends not only on the modulated potential, but also on the transport properties of electrons and holes. © *2000 American Institute of Physics.* [S0003-6951(01)02701-2]

The dynamics of photogenerated carriers in semiconductor structures modulated by periodic electric potentials has received considerable attention in recent years.[1–6] The intrinsic type-II modulation introduced by the potential spatially separates photogenerated electrons (e) and holes (h) and stores them in regions of high (denoted in the following as H regions) and low (L) potential, respectively. The spatial separation substantially increases the lifetime of photogenerated carriers over the radiative lifetime for interband optical transitions in a field-free region. The dynamic control of carrier lifetime makes modulated potentials ideal structures for optical memories based on the storage of electron–hole pairs. Different approaches have been envisaged to realize the potential modulation. Döhler and co-workers and Street *et al.*[3] proposed doping superlattices to create a type-II periodic potential modulation of the form $HLHL$ along the growth direction of GaAs/(AlGa)As structures, which considerably prolonged the carrier radiative lifetime. Lateral electric fields produced by metal gates provide an efficient way of modulating the in-plane electronic properties of quantum-well structures.[7–10] Recently, Zimmermann *et al.*[4] presented a quantum-well (QW) based photonic memory cell based on this approach, where an interdigital gate creates a lateral $HLHL$ superlattice under an applied bias, which can store photogenerated carriers in each HL subcell. Acoustically driven light storage, where the modulated potential is created by the lateral piezoelectric field of a traveling[5] or of a standing surface acoustic wave,[6] have also been proposed.

In this contribution, we directly access the microscopic carrier dynamics in light storage cells, and in particular the role of carrier transport on the storage and recombination processes, by combining spatially and time-resolved photoluminescence (PL) spectroscopy. Previous optical investigations of carrier dynamics used probes with dimensions considerably larger than the modulation period. Information about the microscopic carrier distribution was extracted in an indirect way by comparison with theoretical models. Here, however, we directly detect when and where optically generated carriers are stored and subsequently recombine.

The studies were performed using the interdigital gate pattern illustrated in Fig. 1(a). The gate creates a dynamic lateral superlattice of the type $HHLLHHLL$ in the plane of a GaAs quantum well, when excited by a radio-frequency (rf) voltage $V_{\mathrm{rf}}=V_{\mathrm{rf},0}\sin(2\pi f_{\mathrm{rf}}t+\phi)$, where $V_{\mathrm{rf},0}$, f_{rf}, t, and ϕ are the voltage amplitude, frequency, time and phase respectively. The potential distributions in the QW created by positive ($t=0,\phi=90°$) and negative ($t=0,\phi=-90°$) biases are shown in Fig. 1(b). In a HH cell, there exists a local potential minimum (maximum) in position A for positive (negative) voltages, which can trap holes (electrons). In a HL cell, however, the potential varies almost linearly between the electrodes, thus indicating that the electric field is approximately uniform at position B. Time-resolved PL measurements demonstrate that photogenerated carriers can be stored both in a HH (or LL) cell (through light excitation in position A between equipotential electrodes) and in a HL cell (excitation between electrodes at different potentials, position B). The carrier dynamics shows distinct behaviors in the two subcells, as expected from the different potential profiles at the two locations. The microscopic measurements unveil additional effects that have escaped attention in previous investigations. The first is the fundamental role of carrier transport on the storage efficiency and on the recombination dynamics. In particular, the difference in mobilities for electrons and holes leads to a strong dependence of the PL dynamics on the phase ϕ of the rf voltage at the arrival

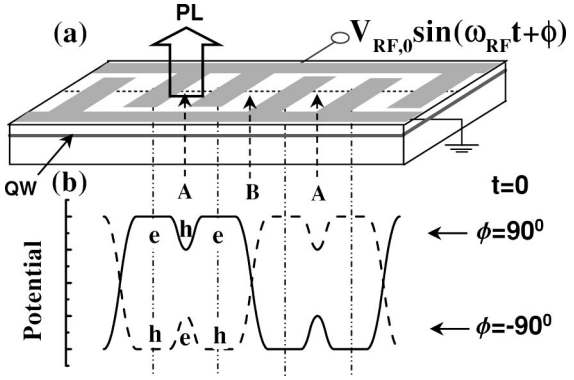

FIG. 1. (a) Structure of the quantum-well sample and (b) schematic potential profile for different applied rf voltages showing the storage locations of electrons (e) and holes (h).

[a]Electronic mail: santos@pdi-berlin.de

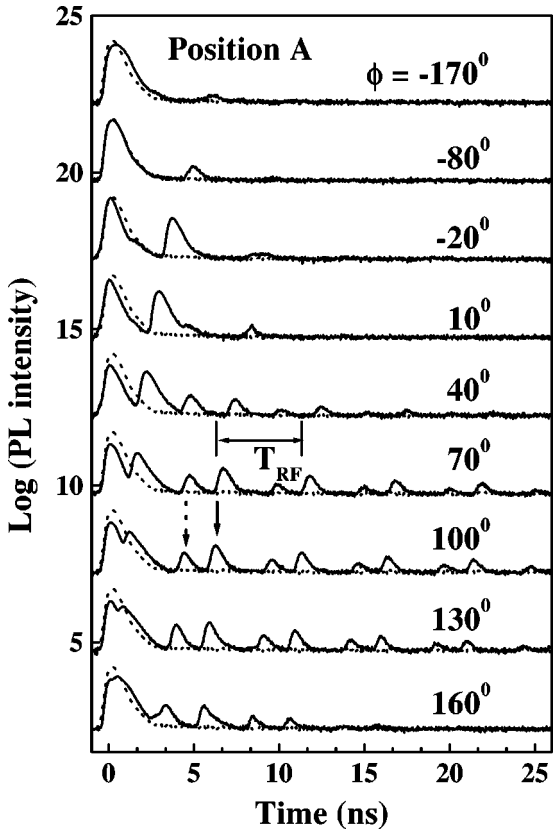

FIG. 2. Time-resolved photoluminescence traces measured at position A for different excitation phases ϕ of the rf field. The PL trace recorded without applied field is superimposed as a dotted line on each trace. The dotted and solid arrows indicate the $h \rightarrow e$ and $e \rightarrow h$ PL pulses for $\phi = 100°$. The traces are shifted vertically for clarity.

time of the laser pulse used to generate carriers. This effect is well reproduced by numerical simulations of the carrier dynamics using a model that takes into account carrier diffusion and drift and under the time-dependent lateral electric fields.

The experiments were performed on a 5-nm-thick $Al_{0.3}Ga_{0.7}As/GaAs/Al_{0.3}Ga_{0.7}As$ QW sample grown by molecular-beam epitaxy. Aluminum was evaporated on the surface to form the split finger gate, shown in Fig. 1(a). The pattern shows a spatial period $\lambda = 14.4\,\mu$m, consisting of 1.8-μm-wide metal lines separated by 1.8 μm. One finger set was grounded, while the other was excited by a high-frequency ac voltage ($f_{rf} = 200$ MHz) with a nominal amplitude $V_{rf,0}$ of about 2 V. Since the QW is located only 55 nm below the surface, the potential modulation at the QW depth is approximately the same as at the sample surface. The PL measurements were performed at positions A and B at 14 K using a confocal microscope with coincident illumination and detection areas with a diameter ρ_0 of about 2 μm. Time resolution was obtained by exciting the PL with a pulsed laser (pulse width of 75 ps at 640 nm) synchronized with the rf generator and using a fast photomultiplier as a detector (time resolution of approximately 0.4 ns). The synchronization allows us to control the phase ϕ of the rf voltage V_{rf} at the arrival time of the laser pulse.

Figure 2 displays the evolution of the QW excitonic PL (photon energy of 1.61 eV) at position A, after pulsed-laser excitation for different phases ϕ. The corresponding PL trace recorded without applied rf voltage is superimposed as a dotted line on each trace. Under a rf voltage, the PL traces show, in addition to the initial PL pulse at $t = 0$, a series of extra pulses (after pulses) with a repetition frequency that depends on the period T_{rf} of the rf voltage. The intensity and the number of the PL pulses depend sensitively on ϕ. The intensity is the lowest for $0° < \phi < 180°$, corresponding to positive rf voltages at the arrival time of the laser pulse. This behavior can be understood by taking into account that holes are less mobile than electrons. For negative rf voltage [corresponding to the situation indicated by the dotted line in Fig. 1(b)], PL suppression requires the extraction of optically generated holes from the generation region by the applied field. This process is less effective than the extraction of electrons, which accounts for the PL suppression under positive voltages.

The most striking feature in Fig. 2 is the appearance of strong PL after pulses for $10° < \phi < 160°$. These PL pulses result from the recombination of carriers stored in the modulated potential, when the rf potential reverses its sign. In order to understand the details of the delayed eh recombination, the carrier dynamics was simulated by solving the drift-diffusion equation for carrier motion under the rf electric field. In the simulations, the potential in the QW was assumed to be constant below the electrodes. Between two electrodes, the potential was assumed to be the same as that produced by two infinite wires with diameter equal to the width of the electrode. The mobilities of electrons and holes were varied in order to reproduce the experimental result. Best agreement was obtained using mobilities of 10^4 and $500\,cm^2/(V\,s)$ for electrons and holes, respectively.

Figure 3(a) compares the calculated PL intensity at position A (dashed line) for $V_{rf,0} = 1.7$ V and $\phi = 40°$ with the corresponding experimental time-resolved PL trace (solid line). The calculated PL was obtained by integrating the recombination rate (assumed to be proportional to the product np of the electron and hole concentrations) over the detection area. The calculated trace reproduces well the experimental results, showing after pulses at time delays of $0.43\,T_{rf}$ and $0.93\,T_{rf}$ (note that the broadening of the PL pulses due to the finite-time resolution was not taken into account in the calculations). The origin of these pulses can be understood by considering the profiles for the potential (dashed lines) and for the concentration of electrons (solid lines) and holes (hollow cycles) for different time delays shown in Fig. 3(b). Immediately after the laser pulse, the photogenerated electrons are stored below the positively biased metal electrodes, while the holes are trapped into the potential minima between the electrodes. The first after pulse occurs just after the rf voltage reverses sign at $t = 0.43\,T_{rf}$: electrons, in this case, return to the detection position A and recombine with the holes stored there. We will label this pulse as $e \rightarrow h$ to stress the fact that electrons are driven to the detection spot A, where the holes were initially stored. The delay time for this first after pulse was used to calibrate the absolute phases ϕ. Only a fraction of the carriers have enough time to recombine before they are separated again when the field reverses for $0.43\,T_{rf} < t < 0.93\,T_{rf}$. Holes are then stored below the metal fingers and electrons at the local potential maximum in between the electrodes [cf. dashed line in Fig. 1(b)]. At t

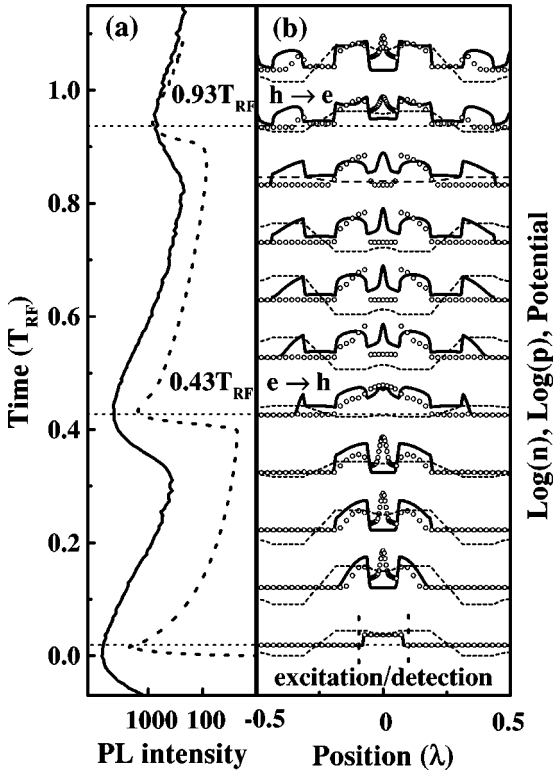

FIG. 3. (a) Measured (solid line) and simulated (dotted line) PL traces for $\phi=40°$. (b) Dependence of the potential (dashed lines) and of the electron (n, solid line) and hole (p, hollow circles) concentrations on position [in units of the period $\lambda=14.4\ \mu$m of the metal gate, cf. Fig. 1(a)], at different times after a pulse excitation (left scale). The position of the electrodes corresponds to the regions of flat potential.

$=0.93\,T_{\mathrm{rf}}$, the holes return to position A and recombine with electrons still present at this position. This recombination process will be denoted as $h\rightarrow e$. The sequence of $h\rightarrow e$ and $e\rightarrow h$ PL pulse repeats at multiples of the time interval $T_{\mathrm{rf}}=5$ ns after the first $e\rightarrow h$ pulse, as illustrated in Fig. 2.

The $h\rightarrow e$ pulses have a lower amplitude as compared with that of the neighboring $e\rightarrow h$ pulses for $40°<\phi<160°$, as indicated by the solid and dashed arrows in Fig. 2. This behavior is attributed to the lower mobility of holes as compared to electrons. During an $e\rightarrow h$ recombination [e.g., $t=0.43\,T_{\mathrm{rf}}$ in Fig. 3(b)], a large density of holes is present in position A when electrons reach this position. For the $h\rightarrow e$ process ($t=0.93\,T_{\mathrm{rf}}$), however, most of the highly mobile electrons have already left position A, when holes arrive there, leading to a weaker PL pulse.

The PL traces from position B show only a few PL after pulses with amplitudes much smaller than for those found for position A. While the high field in *HL* cells leads to an efficient ionization and lateral separation of *eh* pairs, it also prevents carrier recombination at position B, thus leading to weak after pulses. Numerical simulations of the carrier dynamics in this cell (not shown) reveal that most carriers generated in a *HL* cell are driven to the two neighboring *HH* (or *LL*) cells by the strong field, where they recombine.

In conclusion, we have investigated light storage and carrier dynamics in quantum-well structures modulated laterally by high-frequency electric fields. The spatial dependence of the carrier storage and recombination dynamics in these structures depends not only on the intensity of the applied rf field, but also on the transport properties of the photogenerated carriers. The investigation of dynamic effects in these structures is important for operation of microscopic photonic memory cells.

The authors thank H. Grahn and O. Brandt for comments and for critical reading of the manuscript.

[1] G. H. Döhler, Phys. Status Solidi B **52**, 533 (1972).
[2] G. H. Döhler, H. Künzel, D. Olego, K. Ploog, P. Ruden, and H. J. Stolz, Phys. Rev. Lett. **47**, 864 (1981).
[3] R. A. Street, G. H. Döhler, J. N. Miller, and P. P. Ruden, Phys. Rev. B **33**, 7043 (1986).
[4] S. Zimmermann, A. Wixforth, J. P. Kotthaus, W. Wegscheider, and M. Bichler, Science **283**, 1292 (1999).
[5] C. Rocke, S. Zimmermann, A. Wixforth, J. P. Kotthaus, G. Böhm, and G. Weimann, Phys. Rev. Lett. **78**, 4099 (1997).
[6] P. V. Santos, M. Ramsteiner, and R. Hey, Phys. Status Solidi B **215**, 253 (1999).
[7] S. Zimmermann, A. O. Govorov, W. Hansen, and J. P. Kotthaus, Phys. Rev. B **56**, 13414 (1997).
[8] M. Hagn, A. Zrenner, G. Böhm, and G. Weimann, Appl. Phys. Lett. **67**, 232 (1995).
[9] H. Drexler, W. Hansen, S. Manus, J. P. Kotthaus, M. Holland, and S. P. Beaumont, Phys. Rev. B **49**, 14074 (1994).
[10] A. Schmeller, W. Hansen, J. P. Kotthaus, G. Traenkle, and G. Weimann, Appl. Phys. Lett. **64**, 330 (1994).